



Modeling the Effects of Land Use Change on the Water Temperature in Unregulated Urban Streams

Robert T. LeBlanc*, **Robert D. Brown†** and **John E. FitzGibbon†**

**Faculty of Environmental Design, The University of Canberra, PO Box 1, Belconnen, Australia, ACT 2616 and †School of Landscape Architecture, University of Guelph, Guelph, Ontario, Canada, N1G 2W1*

Final version received 4 November 1996; accepted 11 November 1996

Streams, in their natural state, are typically diverse and biologically productive environments. Streams subject to urbanization often experience degradation brought about by the cumulative effects of flow alteration, unsanitary discharge and channelization. One of the water quality parameters affected by urbanization is stream temperature. This study offers a model for predicting the impact of land use change on the temperature of non-regulated streams during extreme events.

A stream temperature model was created by considering the gains and losses of thermal energy resulting from radiation, convection, conduction, evaporation and advection. A sensitivity analysis showed that out of 14 variables, shade/transmissivity of riparian vegetation, groundwater discharge, and stream width had the greatest influence on stream temperature. These same three variables are highly influenced by land use. Individual component models were developed to predict how urbanization changes stream width and baseflow discharge. Using 3-D computer modeling, a model was also developed to illustrate the effects of altering the extent and composition of riparian vegetation on streams with different orientations.

By modeling these three variables as a function of urbanization, the results became inputs into the stream temperature model. The critical urban stream temperature model (CrUSTe), an aggregation of these four models, allows the prediction of stream temperature change as a result of amount, type and location of urbanization within a watershed. It has the potential to become a valuable tool for environmental managers.

© 1997 Academic Press Limited

Keywords: stream temperature, watershed urbanization, riparian vegetation, baseflow, channel morphology.

1. Introduction

The way in which land is developed can seriously compromise the integrity of rivers and streams. Countless studies have focused on the relationship between land use

* Corresponding author. E-mail: rob.leblanc@ns.sympatico.ca

change and the quality and quantity of water in urbanizing basins. These studies suggest that hydrologic changes in urban watersheds can most often be attributed to the modification of stream characteristics which govern discharge, stream chemistry, stream/floodplain interactions and channel morphology. As a result, urbanization is thought to cause reduced baseflows, increased frequency and magnitude of peak discharges, increased sediment loads, reduction in channel and floodplain complexity and impaired water quality (Dunne and Leopold, 1978; Klein, 1979; Halyk *et al.*, 1991).

One of the more significant water quality parameters affected by urbanization is water temperature. Temperature is a major regulator of living systems. Water temperature has been considered one of the most important factors determining the geographic distribution, growth rate and survival of fish and other aquatic organisms (Barthelow, 1989; Holmes and Regier, 1990; Armour, 1991). Temperature regimes are thought to influence migration patterns, egg maturation, incubation success, inter- and intra-specific competitive ability and resistance to parasites, diseases, and pollutants (Armour, 1991). Water temperature also influences the rates of in-stream chemical reactions, the self purification capacity of streams and their aesthetic and sanitary qualities (Feller, 1981). In essence, drastic alterations of the natural temperature regime can cause a cascade whereby the aquatic system can digress from a stable state (with a high assimilative capacity) to an unstable state (with a low assimilative capacity).

1.1. URBANIZATION AND STREAM TEMPERATURE CHANGE

In a study of urbanization and its effect on the temperature of streams on Long Island, New York, Pluhowski (1970) found that modification of the hydrologic environment due to urbanization increased the average stream temperature in summer by as much as 5–8°C. Klein (1979) documented similar changes to the natural stream temperature regime as a result of urbanization.

This paper presents a Critical Urban Stream Temperature (CrUSTe) model which includes the mechanisms by which the critical water temperatures of unregulated streams are affected by land uses within the basin. There were two main reasons for choosing unregulated systems. First, temperature is a function of discharge; so regulated streams (streams with a controlled discharge), by their very nature, have a regulated temperature regime. Daley and Seaders (1966) provide insight into predicting temperatures of regulated systems. Second, and more importantly, the indirect processes that define how stream temperatures are affected by urbanization are not well understood.

“Critical” stream temperatures refer to summer extremes usually associated with low flow periods. It is during these times that the biotic potential of the stream is most at risk. In light of recent global warming predictions (Hengeveld, 1990) and the continuing expansion of urban areas world wide, this study offers valuable insight into stream temperature changes within the context of the developing basin.

Stream temperature is a function of many variables, some of which are directly or indirectly affected by urbanization. This study has identified three main urban factors responsible for altering the thermal environment of streams. These are: (1) changes to the composition of vegetation in the watershed (more specifically, the clearing of riparian vegetation along stream banks), (2) changes to the low flow regime, and (3) changes to the stream’s hydraulic geometry.

Riparian vegetation controls the stream’s thermal character by intercepting short-wave radiation during the day and insulating the stream from long-wave radiation loss at night. Stream discharge also regulates water temperatures. The more water, the more

energy it takes to heat it. The hydraulic geometry, a function of the cross-sectional shape of the stream, influences the surface area of the stream. Since most energy exchanges occur at the air–water interface, the surface area of the stream is directly related to water temperature changes.

To predict how urbanization affects temperature, it is first necessary to model how urbanization influences each of these three variables. Once this is known, the outputs from the individual component models become the inputs into the stream temperature model. This paper is organized in such a way as to present the stream temperature model and each of the three component models (namely, the riparian vegetation removal model, the stream morphology model and the baseflow model). The combination of the component models and the stream temperature model form the basis for the CrUSTe model.

The aforementioned urban variables are not the only variables that can influence water temperature in the urban environment. Other factors not considered by this study include the removal or introduction of wetlands, ponds or lakes, thermal discharge from industrial (or point source) operations, and non point-source thermal discharges (such as storm sewers, urban runoff, agricultural drainage tiles, etc.). The rationale for excluding the first two factors stems from the fact that they are specific to certain watersheds. This study is limited to more generic urban watersheds. The effects on stream temperature resulting from the creation or removal of wetlands is a possible area for further research. Non point-source thermal discharges, having variable heat budget contributions during and after storm events, have been excluded because there is little or no impact on stream temperature during critical periods (which occur during dry periods).

2. Stream temperature model

A physical process model, which estimates the energy inputs and outputs and translates these into temperature changes, was adopted for this study. Although more complex than a regression type model, the physical process model provided a more robust picture of stream temperatures in an urban setting.

The model defined the energy balance in a stream by estimating the radiation, evaporation, conduction, convection and advection in terms of their respective flux densities. The energy balance equation takes the form shown in Equation (1):

$$\Delta H = H_{NR} + H_E + H_C + H_H + H_A \quad (1)$$

where ΔH is the net change in energy stored ($J/cm^2 \cdot hr$), H_{NR} is the net thermal radiative flux, H_E is the evaporative flux, H_C is the conductive flux, H_H is the convective flux, and H_A is the advective flux. For energy gained by the stream, the sign convention is positive. A net increase or decrease in heat results in a corresponding change in water temperature.

The net change in energy stored is translated into a corresponding water temperature change using the specific heat capacity of water ($4184 J/l \cdot ^\circ C$). The equation takes the form:

$$\Delta T = (\Delta H \cdot A / Q) \cdot 0.000664 \quad (2)$$

where ΔT is the change in water temperature ($^\circ C$), A is the stream surface area (m^2)

obtained by taking the product of the reach length and the average reach width, Q is the discharge (l/sec) and 0.000664 is a constant having the units ($1^\circ\text{C}/\text{J}$).

The following sections (2.1–2.5) describe the equations which can be used to obtain values for the five respective energy fluxes.

2.1. H_{NR} , NET RADIATIVE FLUX

The net radiative flux is composed of net short-wave and net long-wave radiation, such that $H_{NR} = R_{S.net} + R_{L.net}$ in W/m^2 .

The net short-wave radiation ($R_{S.net}$) is a product of the short-wave radiation at the stream surface (R_s) and the absorptivity of the water ($1 - \alpha$), such that

$$R_{S.net} = R_s \cdot (1 - \alpha); \text{ where } \alpha = \text{the albedo of water} \quad (3)$$

The reflectivity of the water's surface, or albedo, can be estimated (Anderson, 1954) by:

$$\begin{aligned} \alpha &= 1.18 \cdot \beta^{-0.77} \text{ for } \beta \geq 1.24^\circ; \\ \alpha &= 1.0 \quad \text{for } \beta < 1.24^\circ; \text{ where } \beta \text{ is the solar elevation angle in degrees} \end{aligned} \quad (4)$$

The short-wave radiation received at the stream surface can be calculated from:

$$R_s = (SVF \cdot (0.1 \cdot K)) + (S_f \cdot Trans \cdot (0.9 \cdot K)) + ((1 - S_f)(0.9 \cdot K)) \quad (5)$$

where S_f is the average percent of shade striking the surface of the stream per hour throughout the entire reach. SVF is the sky view factor (as a decimal). The sky view factor is a ratio of the amount of sky visible from a certain point on the surface of the water relative to the maximum possible. If the point is completely enclosed the SVF equals 0, whereas if the sky is completely visible from a point the SVF approaches unity. K is the measured short-wave radiation in the open (W/m^2). The K value can be directly measured using a pyranometer, or it can be estimated from Equation (6) (Brown and Gillespie, 1990). The variable, $Trans$, is the transmissivity of the riparian vegetation (as a fraction) which represents the percent of short-wave radiation which can penetrate the canopy. The transmissivity values for several hydrophilic species of trees have been reported by McPherson (1984).

$$K = (0.77) \cdot (1360) \cdot \text{Sin}(\beta) \quad (6)$$

All objects emit long-wave radiation. The atmosphere and riparian trees are major contributors. The net long-wave radiation ($R_{L.net}$) can be estimated using the net long-wave radiation received at the stream surface (R_L) in W/m^2 and the temperature of the stream (T_w) in Kelvin ($^\circ\text{C} + 273.15$) shown in Equation (7). Since it is the purpose of the model to predict water temperature, a non-steady state (dynamic) approach is needed to solve $R_{L.net}$.

$$R_{L.net} = R_L - 0.98 \cdot (5.67 \times 10^{-8} \cdot T_w^4) \quad (7)$$

R_L is the sum of the long-wave radiation from the sky (L_s) and the trees (L_T) so that

$R_L = L_S + L_T$. L_S and L_T can be approximated by using Equations (8) (Swinbank, 1963 and Monteith, 1973) and (9) respectively.

$$L_S = ((1 - C_C)(1.2 \cdot 5.67 \times 10^{-8} \cdot T_A^4) - 171) + (C_C \cdot (5.67 \times 10^{-8} \cdot T_A^4 - 9) \cdot SVF) \quad (8)$$

$$L_T = (0.98 \cdot (5.67 \times 10^{-8} \cdot T_A^4))(1 - SVF) \quad (9)$$

Where T_A is the temperature of the air in Kelvin and C_C is the cloud cover ratio that ranges from 0 (no clouds) to 1 (completely clouded sky). The units of the net long-wave and short-wave radiation are in W/m^2 . To convert W/m^2 to $J/cm^2 \cdot hr$ for use in Equation (2), it is necessary to multiply W/m^2 by 0.36.

2.2. H_E , EVAPORATIVE FLUX

Evaporative heat transfer results from the change in state of water from a liquid to a vapour. Heat can be dissipated from the stream as energy is supplied to the process of evaporation. Evaporative heat transfer can be approximated using Equation (10) (Krajewski *et al.*, 1982).

$$H_e = -23.42 \cdot W[(1.0646)^{T_w} - (1.0646)^{T_w} h_r] \quad (9)$$

Where W is the wind velocity (m/s) at the surface of the water and h_r is the relative humidity (%) which can be obtained at a local weather station. Due to air turbulence at the surface of the water, the wind velocity value is seldom less than 1 m/s (Krajewski *et al.*, 1982).

2.3. H_C , CONDUCTIVE FLUX

The heat input as a result of conduction was so negligible that it was not considered a significant variable for this study. Conduction may figure into the model if the stream under investigation was very shallow, exposed to direct sunlight and possessed a dark bottom material with a high thermal conductivity (Brown, 1969).

2.4. H_H , CONVECTIVE FLUX

Convection occurs between the water and the air as the energy is transported between the two phases. The catalysts for the convective transfer of energy include the temperature gradient between the air and the water interface ($^{\circ}C$), the atmospheric pressure, p (kPa) and the wind speed (m/s) such that,

$$H_H = 0.0228 \cdot p \cdot W(T_A - T_w) \quad (\text{Krajewski, 1982}). \quad (10)$$

2.5. h_A , ADVECTIVE FLUX

Advection occurs when water (or any substance) at a different temperature is added to the stream. This might occur as tributary inflow, overland flow, direct precipitation or groundwater infiltration. To eliminate complexity in the modeling process, it is best to choose a reach that has no additional tributary inflow (otherwise a continuous measure of temperature, discharge, etc. is required for each tributary). The optimal period for

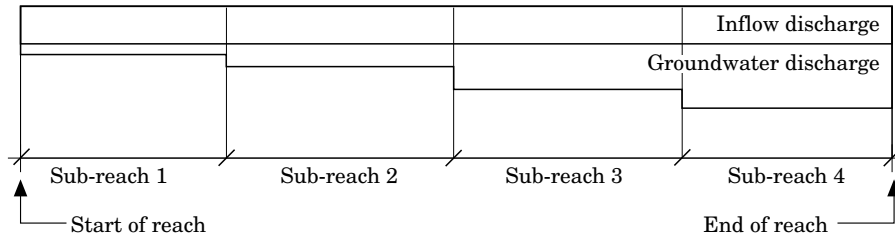


Figure 1. Cross-section of groundwater discharge as interpreted for use in the CrUSTe model. Each sub-reach is modeled individually and sum of the relative temperature changes represents the temperature change of the entire reach.

study is when precipitation and overland flow are negligible. This leaves groundwater flow as the primary advective input.

Groundwater discharge is a typical occurrence in Southern Ontario. If the amount of discharge and temperature of the groundwater is known, a simple temperature–dilution ratio can be used to estimate the water temperature change. In this case, the advective flux density need not be computed.

One approach taken by researchers to determine the influence of groundwater on stream temperature is to attribute the groundwater discharge to the beginning of the reach and assume complete mixing (Meisner, 1990). In this case, an inflow and groundwater discharge ratio is used to calculate a new mixed inflow temperature and discharge, the result of which is used for the temperature model. This may be appropriate for situations when the inflow to groundwater discharge ratio is high, but when the groundwater discharge begins to approach or surpass the inflow discharge, such an assumption will not give accurate results. This approach also has limitations over longer reaches (greater than 1 km).

To overcome this problem, the reach was divided into several sub-reaches, where a proportion of groundwater is attributed to the beginning of each sub-reach. The model is used to calculate the temperature change over each sub-reach with the temperature output of the previous sub-reach becoming the input to the next sub-reach (see Figure 1).

This method assumes that the rate of groundwater infiltration is distributed evenly over the length of the reach. There are limitations to this approach, but if the location and amount of groundwater is known for a specific reach, it would be a simple matter to re-allocate the true discharge proportions to each of the sub-reaches.

2.6. MODEL CONSTRUCTION AND VALIDATION

Upon observation of the various energy balance equations used to calculate stream temperature, it is evident that there are interdependencies built into the model. For example, water temperature (T_w) is required to solve Equations (7), (9) and (10), yet water temperature is the final state variable that the model is trying to predict. Because of this, a dynamic modeling approach is required. STELLA II (High Performance Systems), a commercial dynamic modeling software package, was used to construct the stream temperature model. Using STELLA II's feedback loop capabilities, the water temperature at the end of each sub-reach can be fed back into the equations that

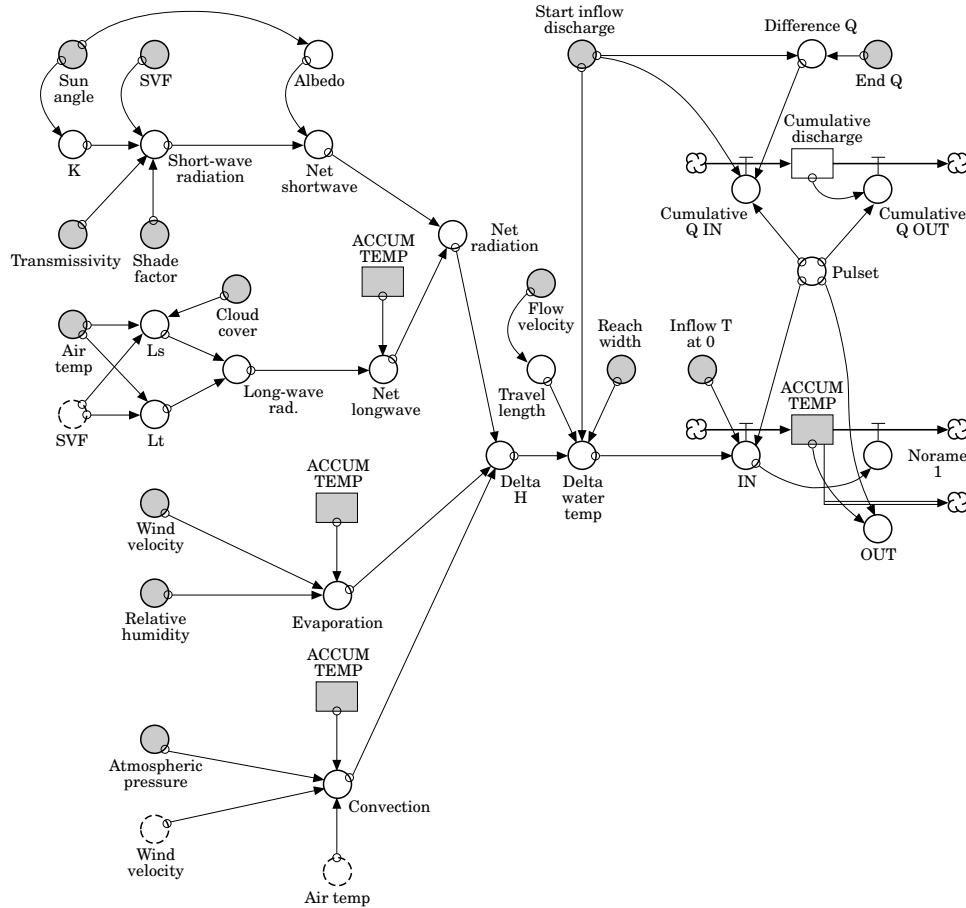


Figure 2. Form of the Stream Temperature Model as constructed in STELLA II. (Dark circles indicate input variables, grey boxes indicate predicted temperatures.)

require water temperature as a variable in the proceeding sub-reach. Figure 2 shows STELLA II's graphical form of the model.

The model was validated using temperature, hydrologic and meteorological data collected from Morningside Creek, just outside of Toronto, Ontario. Figure 3 shows the agreement of the modeled and actual results over a two day period in August, 1994. The standard error of estimate ($S_{y,x}$) over the two day period is 0.77°C. Generally, there was good agreement between the modeled and the actual results.

3. Sensitivity investigation

A sensitivity investigation was performed to gauge the model's sensitivity to its various parameters. The sensitivity investigation helped to: (a) identify the parameters that were sensitive and insensitive, (b) ascertain the degree to which reliable measurement was warranted, (c) validate the model's consistency with the real world system under investigation (Reckhow and Chapra, 1983).

The details of the sensitivity investigation approach can be found in LeBlanc (1994).

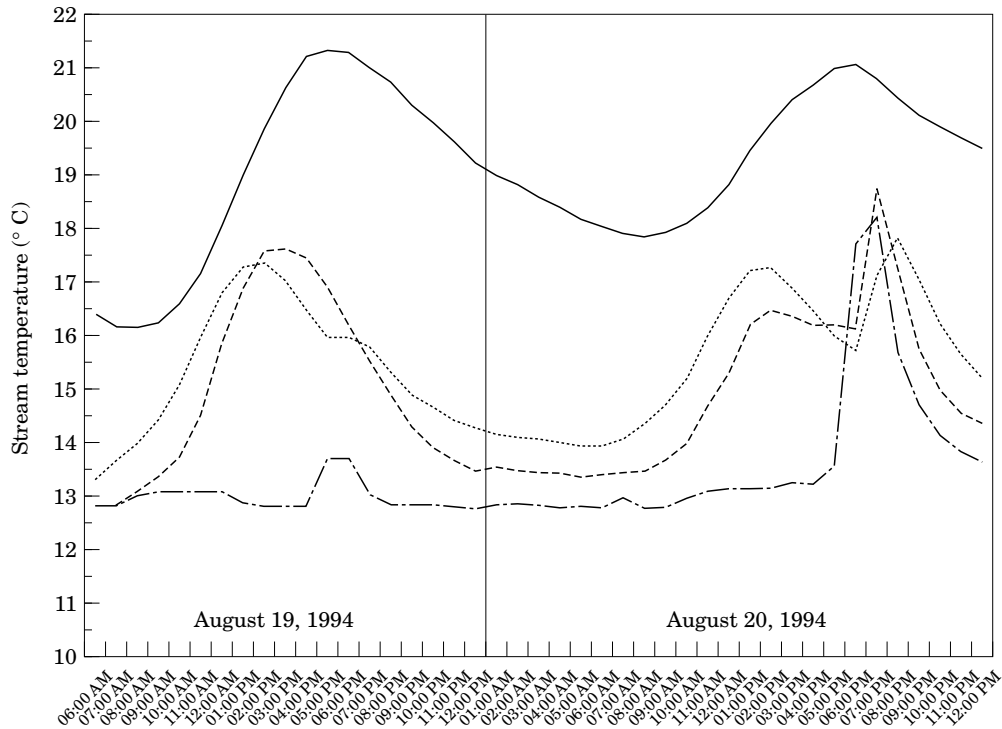


Figure 3. Predicted vs actual stream temperatures for Morningside Creek, Ontario, August 1994. (—) inflow temperature, (---) outflow temperature, (.....) predicted outflow temperature, (-·-·-) groundwater temperature.

From the resultant descriptive statistics, a box plot was constructed to show the relative influence of each variable on stream temperature (Figure 4). The box plot shows the relative influence of each parameter on water temperature. From the sensitivity investigation, discharge was found to have the largest influence on stream temperature. Sun angle, transmissivity of vegetation and groundwater discharge also had a significant influence on the stream temperature. It is important to realize that these findings are representative of the input parameters chosen and can vary depending on how the parameters change in each geographic region.

3.1. ESTIMATING THE DEGREE OF RELIABLE MEASUREMENT

To estimate the accuracy and precision of measurements required in the model, the values of representative input parameters were raised and lowered until a stream temperature change of 0.5°C was observed. "Representative" input parameters are values that might be expected in the local region under investigation (in this case, southern Ontario, Canada). Extreme events (i.e. those events that contribute to high stream temperatures) were chosen because it is during these times when the model's resolution would be at its greatest.

Once representative data were collected (see LeBlanc, 1994, for more details) and run through the stream temperature model, the suggested degree of reliable measurement per 2 km of reach was determined for each parameter. From these data it was apparent

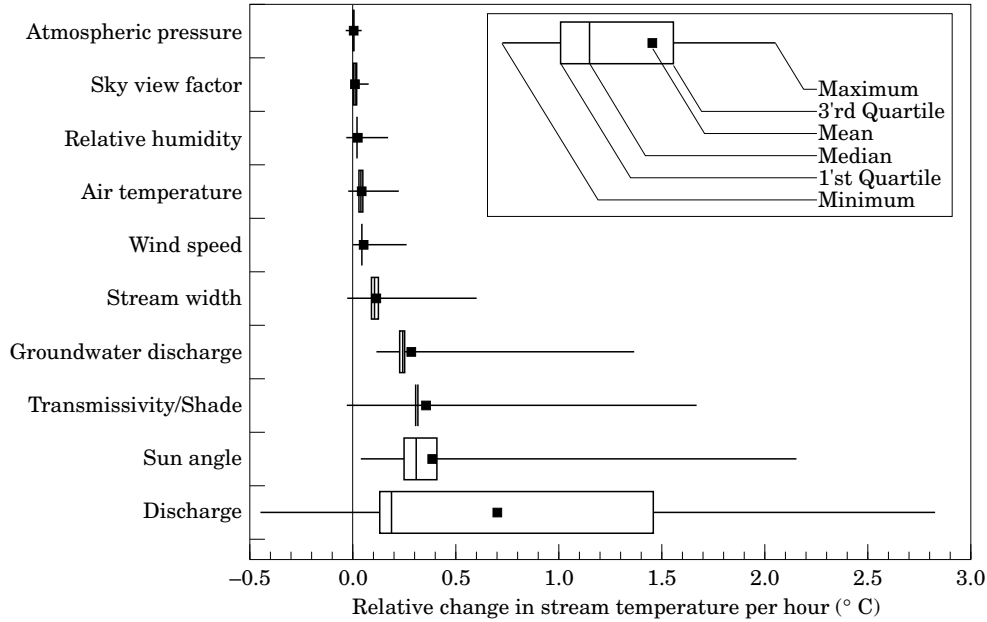


Figure 4. Box plot of the relative sensitivities of each parameter per hour, taken from the descriptive statistics for each parameter.

TABLE 1. Representative data for southern Ontario and the corresponding degree of reliable measurement

Parameter	Representative data	Degree of reliable measurement	Other parameters used in the model
Sun angle	70.1 ^{oa}	8.1°	Stream length 2 km
Sky view factor	0	±1	Groundwater temperature 8.3°C
Transmissivity	1	0.07	Inflow temperature 14°C
River discharge	8 l/s	14 l/s	
Groundwater discharge	79 l/s	5.7 l/s	
Stream width	2.1 m	0.14 m	
Wind speed	4.2 m/s	4.8 m/s	
Air temperature	26.1°C	3.5°C	
Relative humidity	59%	17%	
Atmospheric pressure	98.68 kPa	70.7 kPa	

^a Maximum possible sun angle on 21 June, in Waterloo, Ontario, Canada.

that the sky view factor and the atmospheric pressure would require only estimated values as inputs since the degree of reliable measurement almost equalled the parameter's representative range. The representative data and an estimate of the degree of reliable measurement are summarized in Table 1.

The values having the smallest proportional degree of reliable measurement (the largest influence on stream temperature) included sun angle, transmissivity, stream width and groundwater discharge. Three of the four sensitive parameters, transmissivity,

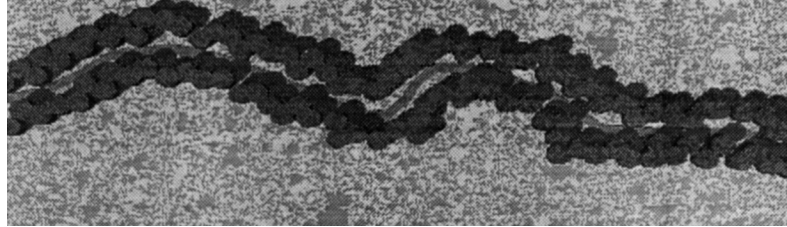


Figure 5. A sample, 3-D model of the east–west oriented stream model at 2:00 pm, early July.

stream width and groundwater discharge, are susceptible to change by urbanization (sun angle is not affected by temperature). It is these three parameters that were modeled in more detail as component models. The next three sections (4, 5 and 6) describe these component models.

4. Component model 1: removal of riparian vegetation

The sensitivity investigation revealed that solar radiation was one of the most influential meteorological variables in the stream temperature model. The composition and extent of riparian vegetation, in turn, had a major influence on the radiation received and lost from the stream surface. Consequently, water temperature is very sensitive to stream shading. There is a great deal of literature describing the effects of vegetation on stream temperatures (Brown, 1969, 1970; Klein, 1979; Feller, 1981; Barton *et al.*, 1985; Meisner, 1990).

The significance of vegetation results from a tree's capacity to absorb short-wave radiation that would otherwise be absorbed by the stream. Vegetation also helps to moderate cooler stream temperatures at night by emitting more long-wave radiation than open sky and reducing the water's long-wave radiation losses. In addition, the loss of roots, which provide stream bank stability, may lead to long-term cumulative temperature effects as stream geometry is altered (Beschta and Taylor, 1988).

This study limits its investigation of the affects of vegetation removal on water temperature to riparian vegetation and makes the assumption that other vegetation removed in the watershed plays a less significant role. More conclusive research needs to be done to determine the affects of groundwater heating due to interbasin vegetation removal.

Several authors have hypothesized that stream orientation affects the amount of stream shading (Geiger, 1965; Moore, 1967). Pluhowski (1970) estimated that east–west oriented streams received from 7 to 19% more sunshine than north–south streams. Advances in the ease of use of 3-D computer modeling and image analysis can provide accurate estimations of effects of stream orientation and vegetation removal on shade. To test this, a three-dimensional computer model of a typical southern Ontario stream reach was constructed. The model was oriented predominantly east–west, and had a stream width of 2 m, a stream length of 180 m (stream area = 360 m²), and was surrounded by 9 m high riparian vegetation. The model was given the coordinates of a central southern Ontario location (Waterloo, 43°27'N 80°23'W, 314 m) on an early July day (Figure 5). The simulated shade cast on the river was estimated as a percentage of the stream area using image analysis software for each hour of sunshine (using the hourly sun angles at the Waterloo location). Four simulations were run for varying amounts

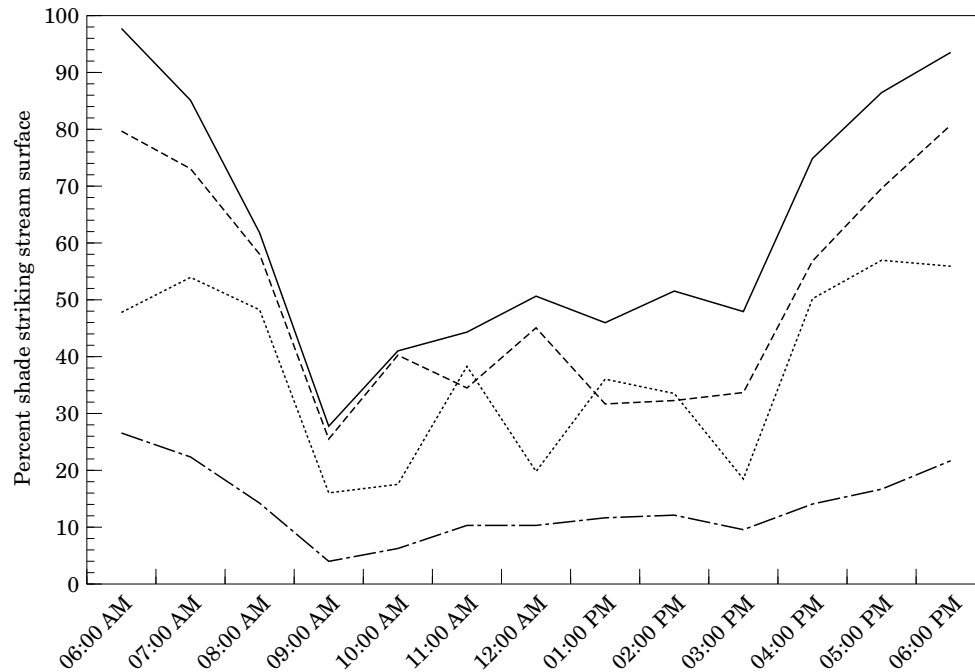


Figure 6. Diurnal shade values for typical east–west oriented streams in Waterloo, Ontario during early July.
% vegetation: — 100%, --- 75%, 50%, -.-.- 25%.

of streamside vegetation (100%, 75%, 50%, and 25% vegetation) to simulate the effects of vegetation removal on shade. Once this simulation was complete, the same model was turned 90° (representing a predominantly north–south oriented stream) and the same procedure was applied. A plot of the percent shade at the stream surface for the east–west oriented stream is presented in Figure 6, while a plot of the same stream turned 90° (north–south oriented) is presented in Figure 7.

Figures 6 and 7 show the effect of stream orientation and vegetation removal on shade. For all vegetation removal scenarios, the shade in the east–west oriented stream (Figure 6) tended to decrease rapidly at sunrise, but stayed at mid range values through most of the day before ascending again at about 3:00 PM. In contrast, the shade on the north–south stream (Figure 7) seemed to stay constant until mid morning, then it dipped very rapidly until noon to below 10% shade (for all vegetation scenarios).

The hourly shade values for both stream orientations became inputs into the CrUSTe model to simulate the influence of stream orientation and vegetation removal on water temperatures for a typical day in central southern Ontario in a typical second order stream.

The diurnal thermographs are shown in Figure 8 for east–west oriented streams and Figure 9 for north–south oriented streams. Again, there were noticeable differences in the impact of stream orientation and vegetation removal on stream temperature. Vegetation removal was shown to increase stream temperatures up to 2°C. It is important to note that these thermographs are representative of a typical groundwater influenced system which tend to moderate extremes of temperatures. Vegetation removal along

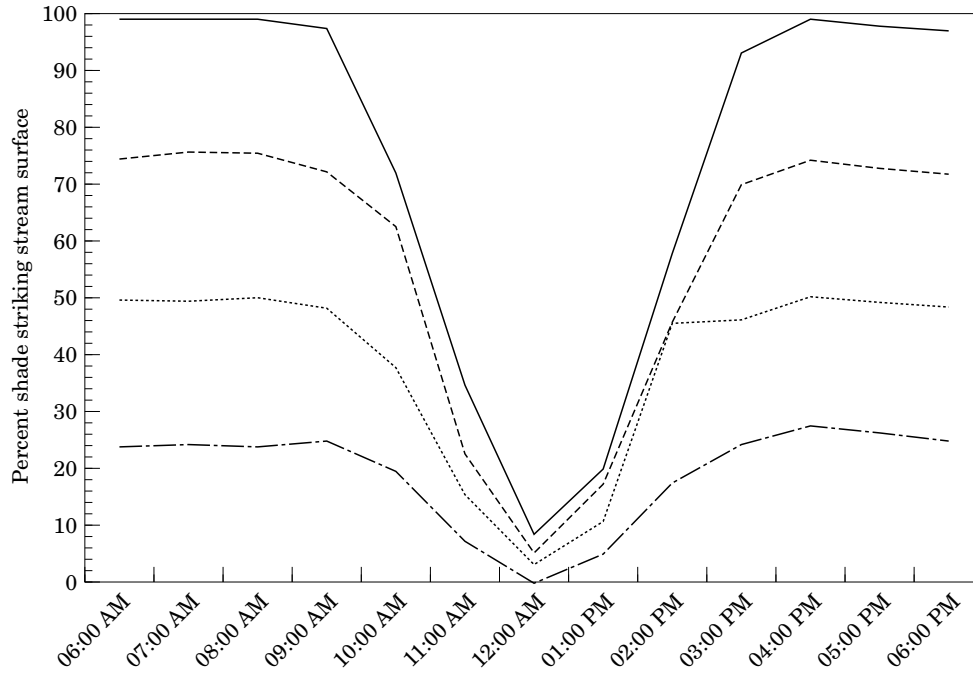


Figure 7. Diurnal shade values for typical north-south oriented streams in Waterloo, Ontario during early July. % vegetation: — 100%, --- 75%, 50%, -.-.- 25%.

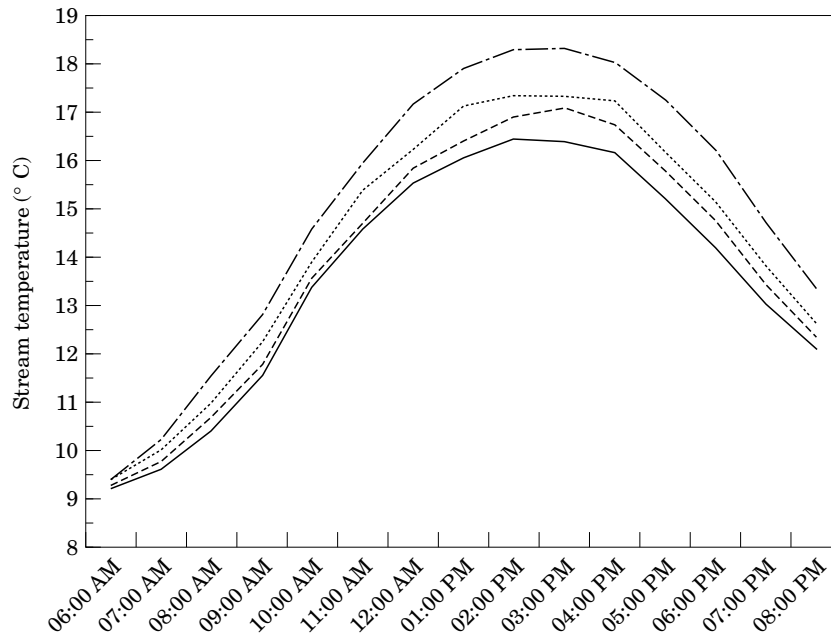


Figure 8. Stream temperature scenario using data generated for typical east-west streams. % vegetation: — 100%, --- 75%, 50%, -.-.- 25%.

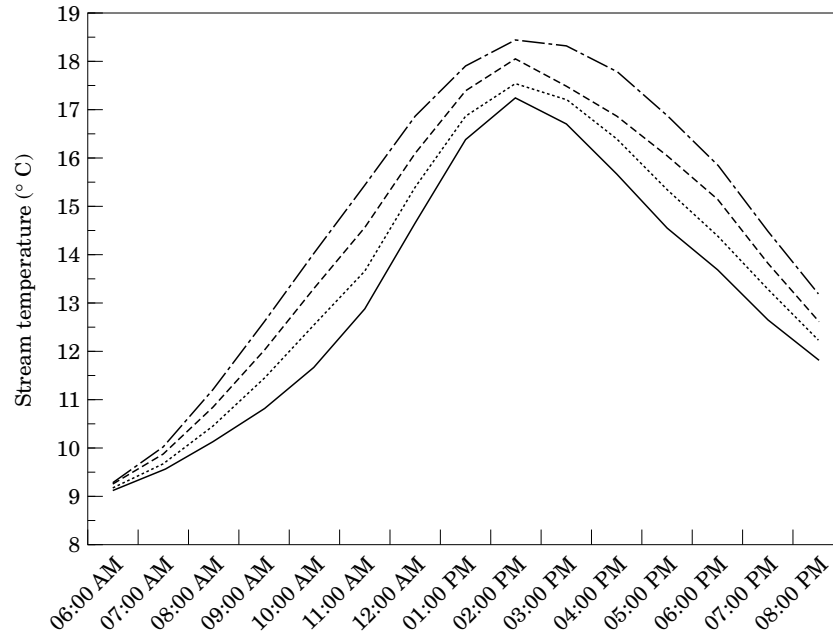


Figure 9. Stream temperature scenario using data generated for typical north-south streams. % vegetation: — 100%, --- 75%, 50%, -·-·- 25%.

streams lacking such groundwater moderation could have a much more pronounced influence on stream temperature.

In comparing the effects of stream orientation on stream temperature, the thermographs showed that while north-south oriented streams were typified by higher maximum temperatures (all other things being equal), east-west oriented streams tended to retain their maximum temperature over a longer period of time. In other words, the north-south streams had a greater maximum intensity, but the east-west streams had a longer maximum duration. Both intensity and duration of water temperatures play an important role in determining a fish's thermal tolerance. Armour (1991) presents a model for evaluating and recommending temperature regimes to protect fish.

4.1. EFFECTS OF DIFFERENT TREE TYPES ON STREAM TEMPERATURE

Canopy transmissivity, a measure of the tree's density, was also found to influence stream temperature. To visualize the impacts on stream temperature resulting from the removal of different vegetation types, two types of trees (with widely different transmissivity values) were chosen for comparison. These trees and their respective transmissivity values were *Acer saccharinum* ($T=0.11$, McPherson, 1984) and *Gleditsia triacanthos inermis* ($T=0.30$, McPherson, 1984). Values for the other model parameters were similar to those used in Section 4.

The results of the simulation indicated that, as more vegetation was removed, the thermographs for both transmissivity types became more similar. This trend stems from the decreasing significance of transmissivity as more and more vegetation is removed. Conversely, the largest influence on water temperature due to different transmissivity types occurred at 100% vegetation.

For the east–west oriented streams the difference in water temperatures (as a result of the two different transmissivities) was most pronounced from 10:00 AM until about 3:00 PM (i.e. during the period of maximum daily water temperatures). On east–west streams the denser canopy ($T = 0.11$) decreased the overall maximum stream temperature. The difference between the peak temperatures for the two canopy types was about 0.8°C . For the north–south oriented stream the largest difference in water temperatures occurred as the thermograph curve ascended and descended to and from the point of maximum water temperature (i.e. from 8:00 AM to 10:00 AM and 3:00 PM to 5:00 PM). Mid-morning and mid-afternoon temperature differences were from $0.5\text{--}0.7^{\circ}\text{C}$ lower for the denser canopy. However, unlike the east–west oriented streams, the peak stream temperatures for the different canopy types on north–south oriented streams were the same (i.e. the different canopy types did not affect the maximum temperature).

5. Component model 2: channel morphology

Channel width was one of the significant CrUSTe model parameters. The greater the channel width, the greater the surface area for the exchange of radiant, evaporative and convective fluxes. Streams with high width-to-depth ratios would be expected to have greater temperature extremes than streams with low width-to-depth ratios with similar cross-sectional areas.

Researchers attribute channel morphology to discharge, velocity, sediment load, sediment size, channel slope, width and depth (Dunne and Leopold, 1978). A change in any of these characteristics causes disequilibrium and results in the re-establishment of a new channel morphology.

The size and shape of a river were found to be highly correlated with flood frequency and flood intensity. Wolman and Miller (1960) argued that very large floods were too infrequent to shape a channel, while smaller, more frequent floods did not possess the energy required to shape the channel. They concluded that bankfull discharge (the level at which the channel fills completely so that the water is level with the flood plain) is the most effective channel forming flow and that this flow had a recurrence interval of 1.5 years for most rivers.

In many instances, the width, depth, cross-sectional area and velocity can be determined from bankfull discharge (Leopold, 1968; Hammer, 1972; Dunne and Leopold, 1978; Rosgen, 1995). There is considerable consistency among regions. For a large number of basins Dunne and Leopold (1978) found that:

$$\begin{aligned} W &= aQ^{0.50} \\ A &= bQ^{0.90} \\ D &= cQ^{0.40} \end{aligned} \tag{11}$$

Where W , A and D are the width (m), cross-sectional area (m^2) and depth (m) respectively and a , b , and c are coefficients specific to regions. From these equations we can estimate the new stream geometry as a result of a change in bankfull discharge.

To verify these equations and to determine the coefficients and exponents for southern Ontario, a series of rural stream cross-sections dimensions were collected along with their corresponding bankfull discharge. The data were plotted on logarithmic probability paper. The equations that describe these plots are shown in Equation (12).

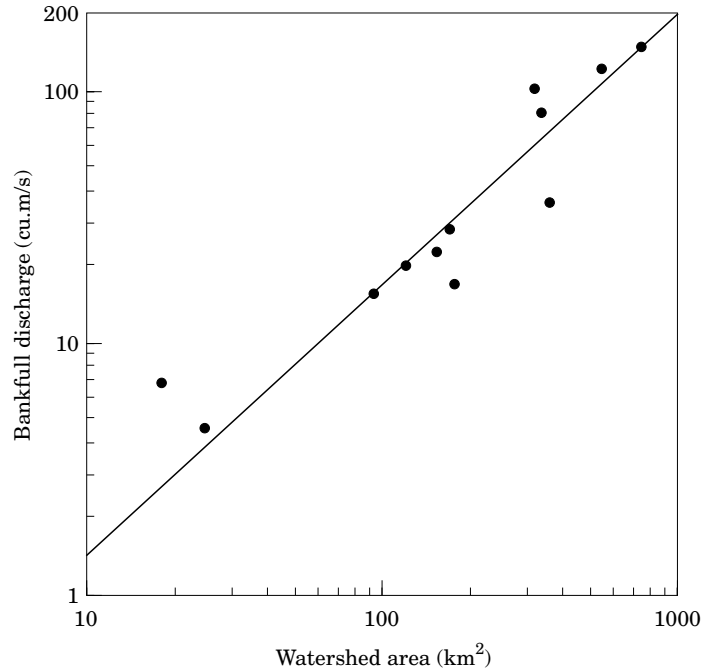


Figure 10. Bankfull discharge ($1Q_{1.5}$) as a function of drainage area for several watersheds in the Grand River Basin, Southern Ontario.

$$\begin{aligned}
 W &= 3.7Q^{0.52} \\
 A &= 1.0Q^{0.84} \\
 D &= 0.27Q^{0.32}
 \end{aligned}
 \tag{12}$$

The value of the equations above is that they describe stream reach geometry in a semi-natural condition. This gives some point of reference from which to compare urbanized streams. Researchers note that the width-to-depth ratio tends to increase with increasing urbanization (Leopold, 1968; Rantz, 1971; Hammer, 1972; Dunne and Leopold, 1978). Since the width exponent (0.52) is greater than the depth exponent (0.32), it is understandable that with increasing discharge, the width will increase faster than the depth (i.e. the width-to-depth ratio increases with increasing bankfull discharge).

“It is a characteristic of river basins that discharge of any chosen frequency of occurrence will increase less rapidly than [watershed] area” (Dunne and Leopold, 1978). A plot of the log (drainage area) versus the log (bankfull discharge) reveals a straight line. To test this for southern Ontario, 12 unregulated, semi-natural (i.e. less than 4% impervious surfaces) sub-basins were chosen from the Grand River watershed. A plot of the drainage area versus the bankfull discharge is presented in Figure 10 ($r^2=0.88$). From this graph, it is possible to estimate the “non-urbanized” bankfull discharge from the drainage area.

Using Equation (12), it is now possible to estimate the effect on the width-to-depth ratio of increasing the bankfull discharge by a given amount. The next step is to determine the increase in the bankfull discharge for urbanized streams.

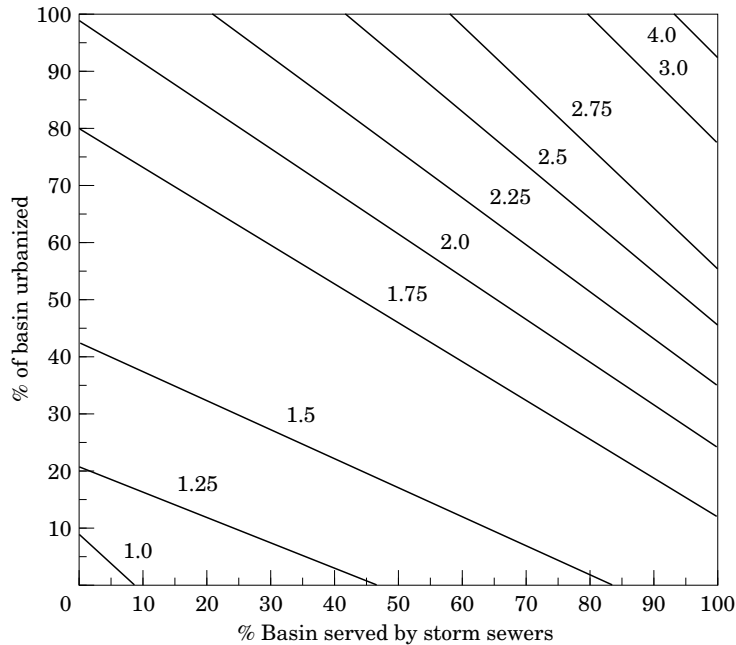


Figure 11. Effect of urbanization and storm sewerage on the 2-year recurrence interval. Family of lines define the ratio peak discharge after urbanization to peak discharge before urbanization. Complete (100%) urbanized is approximately equivalent to 50% impervious surface (after Rantz, 1971. *Suggested Criteria for Hydrologic Design of Storm-Drainage Facilities in the San Francisco Bay Region, California*. United States Geological Survey, Open File Report).

During the process of urbanization the infiltration capacity of the basin is lessened (due to creation of impervious surfaces and the removal of vegetation) and storm sewers are installed. In addition, as the flood plain becomes developed, valuable peak storage space is lost. The consequence of these activities results in a more efficient transmission of the flood wave through channel. This typically causes an increase in the frequency and magnitude of the 1.5 year flood and the concomitant change in channel morphology.

Flood-prediction techniques continue to be developed and refined. Many authors, notably Rantz (1971) and Leopold (1968), have modeled the impacts of development on flood frequency and magnitude. Leopold attempted to determine the magnitude of increase in the mean annual flood (recurrence interval of 2.33 years) resulting from creation of impervious surfaces and installation of storm sewers. Building on this idea, Rantz constructed a series of nemographs which provided a simple, yet effective tool for determining increases in floods of different recurrence intervals from percent urbanization and percent area served by storm sewers. Using Rantz's nemograph at a 2-year recurrence interval (Figure 11), it was possible to estimate the increase in bankfull discharge. Since Rantz's curves were developed for use in San Francisco, California, they were first validated with empirical data for use in southern Ontario.

5.1. STREAM CHANNEL ENLARGEMENT AS A RESULT OF URBANIZATION

By determining the change in the $1Q_{1.5}$ flow (1 day, 1.5 year maximum flow) as a result of urbanization, we can insert this new flow value into Equation (12) to determine the

TABLE 2. Predicted bankfull flows, channel geometry and width enlargement factors for watersheds of different sizes and degrees of urbanization in southern Ontario

Watershed area (km ²)	% urbanized	$1Q_{1.5}$ factor	$1Q_{1.5}$ (m ³ /s)	Expected channel geometry		Width enlargement factor
				Width (m)	Depth (m)	
20	0	0	3	6.55	0.38	1.00
	20	1.31	3.93	7.54	0.42	1.15
	40	1.58	4.74	8.31	0.44	1.27
	60	1.73	5.19	8.71	0.46	1.33
	80	2.20	6.6	9.87	0.49	1.51
50	0	0	7.8	10.77	0.52	1.00
	20	1.31	10.22	12.39	0.57	1.15
	40	1.58	12.32	13.66	0.60	1.27
	60	1.73	13.49	14.32	0.62	1.33
	80	2.20	17.16	16.22	0.67	1.51

new channel width and depth. This provides a good estimate of the new width-to-depth ratio.

It is now possible to estimate the enlargement of the width-to-depth ratio for watersheds of different sizes and varying degrees of urbanization. Table 2 presents a summary of expected channel dimensions in a natural and urbanized condition for different sized watersheds. Included in this table is the expected width enlargement factor for different degrees of urbanization (expressed as a percentage of the impervious area). Since this paper focuses on extreme events (i.e. during baseflow periods), this factor would be multiplied by the natural baseflow channel width to predict the new baseflow width at different stages of urbanization. Notice that the width enlargement factor does not change for watersheds of different sizes. As an example, if the baseflow width of a natural watershed were 2.1 m, then assuming a scenario of 40% urbanization we would expect an enlargement factor of 1.27, and a new channel width of 2.67 m.

Hammer (1972) studied channel enlargement as a result of urbanization but his research concentrated only on the enlargement of channel cross-sectional area. His approach considered the age of the development, breaking down study sites into developments from 0–4, 4–30 and greater than 30 years old, as well as a number of other urban factors. He found that there were notably lower impacts on channel enlargement after 30 years. He hypothesized that “the drainage facilities serving older residential areas may have been relatively poor, either because they were under-designed to begin with or because they had deteriorated over time” (Hammer, 1972).

Hammer’s research implied that developments must be greater than 4 years old to register a channel enlargement change. That is, the width enlargement factor would tend to take at least 4 years to reach an equilibrium after development has ceased.

5.2. STREAM TEMPERATURE CHANGE AS A RESULT OF CHANNEL ENLARGEMENT

To demonstrate the impacts of channel enlargement as a result of urbanization on stream temperature, the scenario of a 10 km² basin undergoing 60% urbanization was considered. At 60% urbanization and 30% storm sewers, one would expect the channel width to enlarge by a factor of 1.33. For a 4 m wide reach at baseflow then, we would

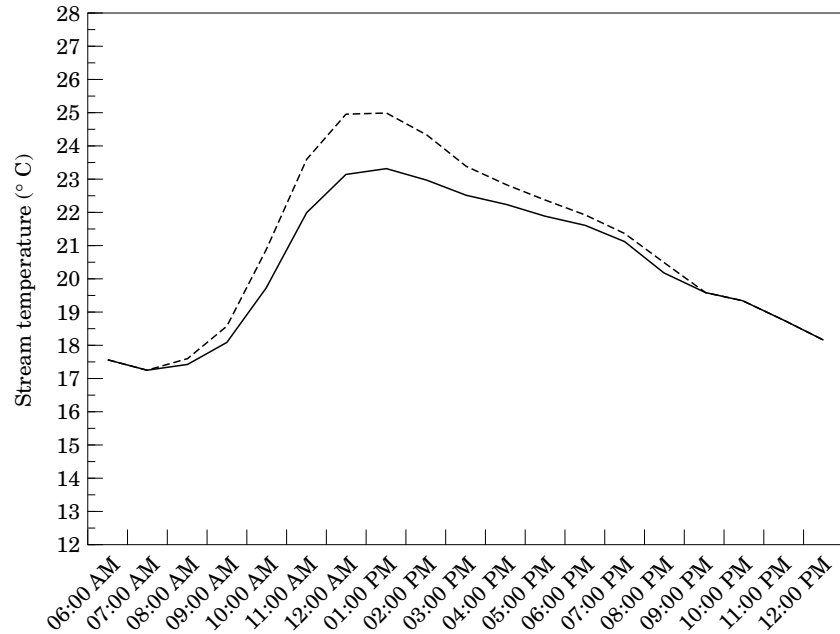


Figure 12. Diurnal thermograph comparing a natural stream to a stream with an enlarged channel geometry as a result of urbanization. (—) non-urbanized, (---) 60% urbanized.

expect the channel to enlarge to 5.3 m. Using representative southern Ontario hydrologic and meteorological data and assuming a north-south oriented stream (at 100% vegetation and transmissivity factor of 0.15) with a 1-h travel time, a diurnal plot of showing the temperature difference between the undeveloped and the developed basin was constructed (Figure 12).

From Figure 12 it is evident that even on a groundwater-influenced stream, the effect of channel enlargement as a result of urbanization can cause a noticeable increase in stream temperatures. The scenario modeled shows a maximum temperature increase of 1.7°C. This is a significant increase considering stream width enlargement is only one of three factors that influence stream temperature increases as a result of urbanization.

6. Component model 3: baseflow character and stream temperature

Inflow discharge and groundwater discharge were found to be highly significant variables in the CrUSTe model. The reason is that the conversion of the various energy fluxes to temperature is inversely proportional to the discharge. Streams or rivers with high discharges would not be expected to exhibit large diurnal temperature fluctuations since it would take a great deal of energy to raise the temperature. Streams with low discharges, on the other hand, might be expected to exhibit high temperature fluctuations. The fact that urbanization can alter the physical character of the groundwater regime has implications on baseflows and, hence, critical stream temperatures.

Urbanization is usually associated with the removal of vegetation within a watershed. Water use by vegetation impacts soil moisture content, groundwater recharge and streamflow. The initial clearing of the land tends to increase the water available for

TABLE 3. $(1 - C)$ values and areas for each of the soil-cover complexes in the D'Aubigny Creek watershed

Land use	Hydrologic soil type											
	A		AB		B		BC		C		CD	
	$(1 - C)$ km ²	$(1 - C)$ km ²	$(1 - C)$ km ²	$(1 - C)$ km ²	$(1 - C)$ km ²	$(1 - C)$ km ²	$(1 - C)$ km ²	$(1 - C)$ km ²	$(1 - C)$ km ²	$(1 - C)$ km ²	$(1 - C)$ km ²	$(1 - C)$ km ²
Woodlot	0.5	0.030	0.44	0.007	0.4	0.535	0.63	0.021	0.24	1.025	0.23	0.098
Long grass	0.45	0.040	0.4	0.026	0.35	0.207	0.28	0.201	0.21	0.12	0.18	0
Lawns	0.4	0.075	0.35	0	0.29	0.354	0.23	0.090	0.17	0.360	0.14	0
Pasture	0.42	0.090	0.38	0	0.35	0.982	0.29	0	0.24	0.686	0.21	0
Row crop	0.34	0.884	0.3	0.234	0.26	3.435	0.22	0.493	0.18	4.931	0.16	0

streamflow by decreasing the rate of evapotranspiration. The effects of vegetation removal on baseflows can vary. In some cases, the reduction in evapotranspiration increases the groundwater table and increases the baseflows. In other situations where precipitation intensity is great, the rain can actually compact the soil to the point where the infiltration potential is reduced and baseflows are lessened. To model the impacts of rainfall characteristics, soil properties, vegetation and land-use on baseflows, the rational runoff method (an equation used to predict peak runoff rates) was refined. Typically, the rational equation takes the form:

$$Q_{PK} = 0.278CIA \quad (13)$$

where Q_{PK} is the peak discharge in m³/s, C is the rational runoff coefficient, I is the rainfall intensity in mm/hr, A is in km².

If the annual catchment water balance is calculated it can be used with a revised form of the rational equation to estimate baseflows. Since C values are an estimation of the proportion of precipitation intercepted, then $(1 - C)$ represents the proportion of precipitation infiltrating the soil. Consequently, Equation (13) can be revised as follows:

$$Q_{BF} = 3.13 \times 10^{-5}(1 - C)(I_p - (I_{ET} + I_i))A \quad (14)$$

where Q_{BF} is the baseflow in (m³/s), I_p is the amount of precipitation (mm/yr), I_{ET} is the rate of evapotranspiration (mm/yr), I_i is the rate of interception (mm/yr) and A is the area in (km²). This equation assumed there are no large water bodies within the catchment, and that there are no regional aquifer recharge zones within the catchment. Regional aquifers can be factored into the water balance for use in Equation (14) if the annual groundwater storage is known.

The model was validated using the D'Aubigny Creek watershed just outside of Brantford, Ontario, Canada. D'Aubigny Creek has a watershed area of 15 km² and is part of the larger Grand River watershed in southern Ontario. The annual rainfall rate of the larger Grand River watershed was 935 mm/yr and had an evapotranspiration rate of 554 mm/yr (Paragon Engineering Ltd, 1992) for the year being simulated. Since a detailed water balance was unavailable for D'Aubigny Creek, these values were used.

Soils and land-use maps of D'Aubigny Creek were digitized and imported into SPANS for spatial analysis. The two maps were overlaid to determine the area of the soil/cover complex. The $(1 - C)$ values and respective areas for the soil-cover complexes in D'Aubigny Creek are shown in Table 3.

TABLE 4. Estimated baseflows (m^3/s) as a function of landscape type and % urbanization (0.5 acre residential sub-division) for a 10 km^2 catchment in southern Ontario, Canada

% Urbanized	Land cover types altered		
	Forest	Meadow	Row crop
0	0.083	0.050	0.030
10	0.077	0.047	0.029
20	0.070	0.044	0.027
30	0.064	0.040	0.026
40	0.057	0.037	0.025
50	0.051	0.034	0.024
60	0.044	0.031	0.023
70	0.038	0.028	0.021

The observed baseflow for June 1991 for D'Aubigny Creek was $0.060 \text{ m}^3/\text{s}$. The predicted baseflow from the model using Equation (14) and the values in Table 4 was $0.045 \text{ m}^3/\text{s}$. From these results, it appears that the baseflow component model has good predictive potential.

6.1. BASEFLOW ALTERATION AND STREAM TEMPERATURE CHANGE

It is impossible to generalize about the effects of urbanization on baseflow. The type of development (extent of impervious surfaces) and the location of the development (i.e. the soil/land cover types being developed over) both play an important role in determining the possible changes in baseflow.

However, in an attempt to determine the impact of land use change on certain landscapes, a methodology was developed to allow some degree of generalization. In essence, what would be useful to environmental managers and planners would be to have an estimate of how certain development types affect baseflows and stream temperatures within the catchment.

Using typical precipitation and evapotranspiration data ($935 \text{ mm}/\text{yr}$ and $554 \text{ mm}/\text{yr}$ respectively) for the Grand River watershed and a standard watershed area of 10 km^2 , a matrix of expected baseflows (assuming no aquifer recharge or large lakes) was created for different stages of urbanization within varying land cover classes (Table 4). Runoff curve numbers from the soil conservation service (1975) were used to determine the C values for forest, meadows, and row crop types (all cover types had a "B" type hydraulic soil group and a "good" hydraulic condition). The type of development modeled was a 0.5 acre (per lot) residential sub-division. Note that the runoff coefficients vary for different land cover types. There may also be some error resulting from assuming a constant evapotranspiration rate across landscape types.

As expected, the baseflows decrease with increasing urbanization. Baseflow reduction rates are most pronounced in forest catchments while the effects of urbanization are less pronounced on pasture and cropland.

Using these baseflow variations as inputs into the stream temperature model it is possible to see the linkages between urban development and stream temperatures as a result of baseflow alterations. The CrUSTe model parameters were set for a north-south

TABLE 5. Estimated peak stream temperatures (°C) as a function of landscape type and % urbanization for a 10 km² catchment

% Developed	Land cover types altered		
	Forest	Meadow	Farm and crops
0	18.52	20.84	20.93
10	18.80	20.86	20.94
20	19.18	20.88	20.94
30	19.54	20.89	20.95
40	20.14	20.90	20.95
50	20.74	20.91	20.96
60	20.88	20.93	20.96
70	20.90	20.94	20.97

oriented stream from 12:00 to 1:00 PM in early July, with a constant inflow of 50 l/s at 12°C and a riparian vegetation transmissivity of 15%.

As a previously forested basin becomes developed, the predicted peak hourly temperature difference between the undeveloped (0%) and 70% developed is about 2.38°C (Table 5). Similarly, for predominantly meadow basins and row crop basins the temperature differences between 0% and 70% developed was 0.10 and 0.04°C respectively. These temperature differences represent average discharge conditions. One would expect that the variation would be more pronounced during dry years when baseflows are lower.

The effect of groundwater withdrawal on the water table is variable within different regions. But due to the sensitivity of groundwater recharge on stream temperatures, any activity which compromises baseflows can have serious repercussions on freshwater stream temperatures.

7. Scenario modeling

The previous component models for vegetation removal, channel morphology change and baseflow reduction can now be aggregated to simulate the impact of urban development on stream temperatures. A step by step approach was adopted to simplify the modeling process. The scenario goes as follows:

A hypothetical rural southern Ontario town is projecting massive growth in the next 20 to 30 years. Within a watershed area of 10 km², provincial and municipal planners are projecting up to 60% urbanization (i.e. 30% impervious area). They expect up to 40% of the watershed to be serviced by storm sewers. Provincial natural resources officials reviewing the projections expressed concern over these figures since the main stream in the basin provides cold water habitat for many thermally vulnerable species including brook trout (*Salvelinus fontinalis*) and Atlantic salmon (*Salmo salar*). Their concern stems from the loss of cold water streams as a result of urbanization in a neighbouring township. In particular they are concerned with a 1 km reach at the outfall of the watershed which provides an excellent spawning ground for fish due to the abundance of cool groundwater inflows and gravel substrate. The province is

interested in predicting the impacts of the proposed development on stream temperatures in the basin.

7.1. STEP 1—BASEFLOW MODELING

Upon digitizing the existing watershed in a geographical information system and using Equation (14) with an annual precipitation rate of 922 mm/year (2-year recurrence interval) and annual evapotranspiration rate of 571 mm/year, a baseflow of 82 l/s was predicted. This figure compared well with the actual baseflow of 76 l/s.

Next, the probable location and type of the new development was digitized and a new soil/cover table was compiled to determine the change in baseflow expected. The predicted new baseflow after urbanization was 50 l/s, a decline of about 60%. The product of 60% and the actual baseflow value gives a value of 46 l/s. This number was used to represent the predicted baseflow value after urbanization. It is assumed that the stream inflow discharge at the beginning of the reach will not change considerably from rural to urban (this is a reasonable assumption for extreme events). This inflow was measured to be 25 l/s.

7.2. STEP 2—VEGETATION REMOVAL

Despite strict environmental protection along the river corridor, it is anticipated that 20% of the riparian vegetation along the 1 km reach would have to be removed due to highway construction and development. A further 5% vegetation might be expected to be lost due to bank undercutting as a result of increased flood flows as a result of urbanization.

Constructing a three-dimensional computer model of the reach, which is predominantly north-south oriented, revealed that the expected shade matched the 75% vegetation for north-south streams in Figure 7.

7.3. STEP 3—CHANGE IN CHANNEL GEOMETRY

Using Figure 10 with a watershed area of 10 km², the anticipated $1Q_{1.5}$ is 1.4 m³/s. Assuming that the Water Survey of Canada has had a gauge on this hypothetical stream for over 20 years, a flood frequency curve of the annual, 1-day maximum discharges can be plotted. The figure of 2 m³/s was observed at the 1.5 year recurrence interval. This compares favorably with the 1.4 m³/s figure obtained from Figure 11.

The width of the stream at bankfull discharge was computed to be 4.4 m from Equation (12). Again this compared favorably with the actual width of 4 m observed from a typical cross-section of the stream. At a site visit during the baseflow period, the stream was surveyed and the wetted width was measured at 3.8 m.

At 60% urbanization and 40% storm sewers, Figure 11 predicts a $1Q_{1.5}$ increase of 1.84 times as a result of urbanization. This gives a new $1Q_{1.5}$ value of 2.6 m³/s. Inserting this value into the width function in Equation (12) yields a new bankfull width of 6 m, an increase of 1.36 times the original predicted stream width. Multiplying this factor by the measured baseflow width of 3.8 m yields a new wetted width at baseflow of 5.2 m.

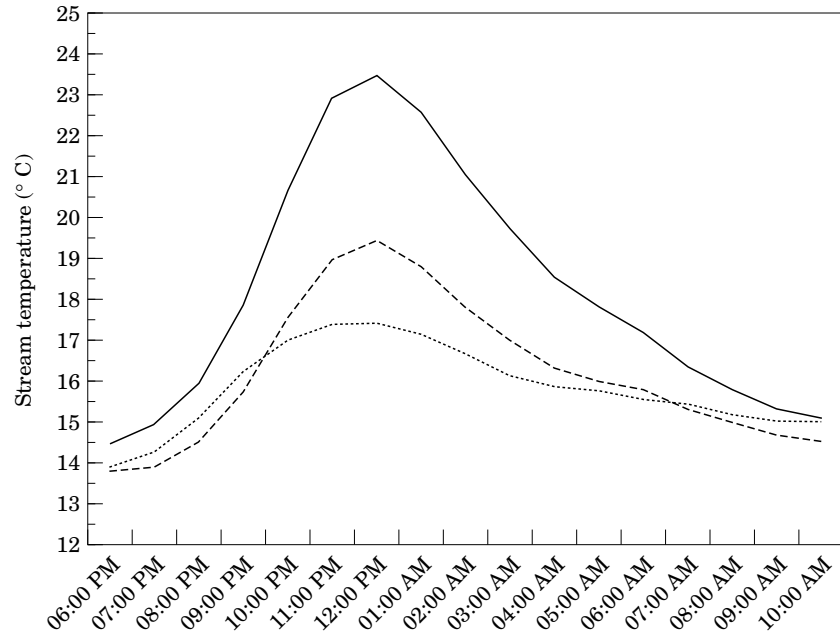


Figure 13. 60% urban vs non-urbanized stream temperatures ($^{\circ}\text{C}$) for a 10 km^2 basin. (—) outflow temperature after 60% urbanization, (---) outflow temperature before urbanization, (.....) inflow temperature at start of reach.

7.4. STEP 4—TEMPERATURE MODELING RESULTS

Steps 1 to 4 have provided all of the necessary model parameters required by the CrUSTe model. The inflow temperatures illustrated in Figure 13 were assumed to be constant for both scenarios (no development and development). This assumption may be a bit misleading since the inflow temperatures in the urbanized scenario could be greater than those in the undeveloped scenario. This is one of the limitations of the model that might be overcome by networking a series of reaches. There are opportunities for further research in this area.

Since the stream velocity at baseflow was 0.27 m/s (i.e. 1 km/hr), Figure 13 need not be calibrated for travel time. From this thermograph, we can see that the model predicts an increase in temperature of almost 4°C . This increase occurred despite the fact that the stream had a large proportion of its flow supplied by groundwater. One might expect a greater temperature difference if the baseflow discharge had been lower. Note also that this modeling exercise considered baseflows at a 2-year recurrence interval. Baseflows at the 10- and 25-year recurrence interval could result in even higher temperatures.

8. Summary and conclusions

This paper has presented a model (CrUSTe) for evaluating the impacts of urbanization on stream temperature. The utility of such a model can be better understood by describing it in terms of the four categories which it encompasses.

- (1) A pro-active tool for landscape planning and environmental management. The

CrUSTe model allows for the assessment of site specific development scenarios before they are constructed to determine the impacts of land-use change on the thermal regimes of streams. For streams with thermally sensitive species, the model can help planners and land managers avoid the destruction of fish habitat. Such predictive capabilities give landscape architects, planners and engineers a new tool for environmental assessment and can help guide development and design decisions.

(2) A reactive tool for stream remediation and rehabilitation. The model provides a mechanism for better understanding the complex interactions between the terrestrial and the aquatic environments. For remediating streams under thermal stress or for re-creating cold water habitat, the model elaborates on the temperature sensitivity of various meteorological, hydrologic and physical parameters. It was found that the most sensitive parameters can be controlled, to some degree, by design.

(3) An educational tool for understanding the historic context of a stream. The model can be used to assess the pre-developed thermal condition of the stream. Such information may be valuable for historic or educational reasons.

(4) A catalyst for further research. The model opens up a variety of possibilities for understanding and predicting the state of urban streams. Since stream temperature is closely related to hydraulic oxygen concentrations, eutrophication, reaction rates, chemical uptake, etc., the model can be used in concert with other models to predict other variables characteristic of urban streams. In addition, since stream temperature affects fish habitat, it must also affect other urban wildlife in the food chain. That is, stream temperature plays an indirect role in determining the capability of the urban corridors to sustain terrestrial wildlife.

The results of this study have implications on how environmental managers, landscape architects and planners go about the planning and design of large-scale urban landscapes. The sensitivity investigation revealed that riparian vegetation, stream width and baseflow discharge (the three variables that can be controlled by design) are significant contributors to stream temperature. As such, any activity (planned or unplanned) that alters these parameters would be expected to alter stream temperature.

References

- Anderson, E. R. (1954). Water loss investigations: Lake Hefner studies. U.S. Department of the Interior, Geol.
- Armour, C. (1991). Guidance for evaluating and recommending temperature regimes to protect fish. Fish and Wildlife Service. Biological Report 90 (22) (Instream Flow Information Paper 27).
- Barthalow, J. M. (1989). Stream temperature investigations: field and analytical methods. U.S. Fish and Wildlife Service. Biological Report 89 (17) (Instream Flow Paper 13).
- Barton, D., Biette, R. and Taylor, W. (1985). Dimensions of riparian buffer strips required to maintain trout habitat in southern Ontario streams. *North American Journal of Fisheries Management* **5**, 364–378.
- Beschta, R. and Taylor, L. (1988). Stream temperature increases and land use in a forested Oregon watershed. *Water Resources Bulletin* **24**, 19–25.
- Brown, G. (1969). Predicting temperatures of small streams. *Water Resources Research* **5**, 68–75.
- Brown, G. (1970). Predicting the effect of clearcutting on stream temperature. *Journal of Soil and Water Conservation* **Jan–Feb**, 11–13.
- Brown, R. D. and Gillespie, T. (1990). Estimating radiation received by a person under different species of shade trees. *Journal of Arboriculture* **16**, 158–161.
- Daley, W. and Seaders, J. (1966). Predicting temperatures in rivers and reservoirs. *Journal of the Sanitary Engineering Division* **February**, 115–133.
- Dunne, T. and Leopold, L. (1978). *Water in Environmental Planning*. New York, New York: W.H. Freeman & Company.
- Feller, M. C. (1981). Effects of clearcutting and slashburning on stream temperature in southwestern British Columbia. *Water Resources Bulletin* **17**, 863–867.
- Gieger, R. (1965). *The Climate Near the Ground*. Cambridge, MA: Harvard University Press.

- Halyk, L., Imhof, J., Johnson, F. and Plank, R. (1991). *Watershed Urbanization and Managing Stream Habitat for Fish*. Transactions of the Fifth-sixth North American Wildlife and Natural Resources Conferences. Edmonton, Alberta: Wildlife Management Institute pp. 269–283.
- Hammer, T. R. (1972). Stream channel enlargement due to urbanization. *Water Resources Research* **8**, 1530–1540.
- Hengeveld, H. G. (1990). Global climate change: implications for air temperature and water supply in Canada. *Transactions of the American Fisheries Society* **119**, 167–182.
- Holmes, J. A. and Regier, H. A. (1990). Influence of temperature changes on aquatic ecosystems: an interpretation of empirical data. *Transactions of the American Fisheries Society* **119**, 374–389.
- Klein, R. (1979). Urbanization and stream quality impairment. *Water Resources Bulletin* **15**, 948–963.
- Krajewski, W., Kraszewski, A. and Grenney, W. (1982). A graphical technique for river water temperature predictions. *Ecological Modeling* **17**, 209–224.
- LeBlanc, R. (1994). A critical event urban stream temperature model for non-regulated urban streams. University of Guelph. Masters thesis.
- Leopold, L. B. (1968). *Hydrology for Urban Land Planning: A Guidebook*. U.S. Geological Survey Circular 554.
- McPherson, E. G. (ed.) (1984). *Energy Conserving Site Design*. Washington D.C.: The American Society of Landscape Architects.
- Meisner, D. (1990). Effect of climate warming on the southern margins of the native range of brook trout, *Salvelinus fontinalis*. *Canadian Journal of Fisheries and Aquatic Sciences* **47**, 1065–1070.
- Monteith, J. L. (1973). *Principles of Environmental Physics*. London: Edward Arnold Ltd, pp. 241.
- Moore, J. E. (1967). *Correlation and Analysis of Water Temperature Data for Oregon Streams*. U.S. Geological Survey Water-Supply Paper, 1819-K:53 p.
- Paragon Engineering Ltd and Ecologists Ltd (1992). *D'Aubigny Creek Master Watershed Plan*.
- Pluhowski, E. J. (1970). *Urbanization and its Effect on the Temperature of Streams on Long Island, New York*. Geological Survey Professional Paper, 627-D.
- Rantz, S. E. (1971). *Suggested Criteria for Hydrologic Design of Storm-Drainage Facilities in the San Francisco Bay Region, California*. United States Geological Survey, Open File Report.
- Rosgen, D. (1994). A Classification of Natural Rivers. *Catena* **22**, 169–199.
- Reckhow, K. H. and Chapra, S. C. (1983). *Engineering Approaches for Lake Management*. Vol. 1: Data analysis and empirical modeling. Boston, MA: Butterworth Publishers.
- Swinbank, W. C. (1963). Long wave radiation from clear skies. *Quarterly Journal of the Royal Meteorological Society* **89**, 339.
- Wolman, M. G. and Miller, J. P. (1960). Magnitude and frequency of forces in geomorphic processes. *Journal of Geology* **68**, 54–74.